Progress In Electromagnetics Research M, Vol. 93, 11–21, 2020

Design of a Dual-Band Antenna System for LTE-M and LTE-MIMO by Exploiting the Characteristic Mode Theory

Kadidiatou Diallo[1, 2, *], Aliou Diallo[1], Ibra Dioum[2], Samuel Ouya[2], and Jean M. Ribero[1]

Abstract—In this article, a compact dual-band antenna system for LTE-M (700–900 MHz) and LTE-2500 dedicated to mobile handsets is presented. The system consists of a dual-band Planar Inverted-F Antenna (PIFA) for LTE-M and LTE-2500 bands where this designed PIFA is frequency reconfigurable in the LTE-M band. Additionally, another PIFA is designed to cover the LTE-2500 band to enable Multiple-Input-Multiple-Output (MIMO) communication for this band. Frequency reconfiguration between 700 MHz and 900 MHz is performed by a varactor diode biased from the RF port using a decoupling circuit to separate DC and RF signals. The compactness of the system and the good isolation between the two antennas were obtained thanks to the study of the characteristic modes of the mobile phone chassis, where the ideal positions of the antennas can be easily obtained. A prototype of our system was fabricated where good frequency reconfiguration and good MIMO performance (TARC and envelope correlation) were achieved.

1. INTRODUCTION

Since the advent of the internet-of-things (IoT) around 2009 [1], this Machine-to-Machine technology which operates in sub-1 GHz frequency bands [2] and using Low-Power Wide-Area (LPWA) networks has become an essential part of our daily lives and will occupy a very important place in the 5G communication. Thus, in the 3GPP (3rd Generation Partnership Project) release's 13, LTE-M (LTE-for-Machines) and NB-LTE (Narrow-Band LTE) are standardized in frequency between 700 MHz and 900 MHz [3–5] and will have to cohabit with the MIMO 4G's current broadband mode standard. Therefore, many multi-band and frequency reconfigurable antennas for telecommunications have been proposed in recent years.

Multi-band or tunable Inverted-F Antennas (IFA) using varactor or Pins diode for LTE-M and other high bands mobile terminal applications were proposed in [6–11]. But the use of IFA antennas forces to leave non-metalized parts on the ground plane, which makes it more sensitive to the environment and to the user's hand than the PIFA antenna. In addition, the use of pin diodes often allows switching only between two bands, unless using multiple pin diodes, which will increase losses and decrease efficiency. The use of varactor diodes on PIFA antennas remains the best option, because with a single active element, we can cover more bands by varying only the DC voltage, while being less sensitive to the environment.

Several authors have proposed frequency tunable PIFA using varactor diode to operate at low frequencies [12–14], but the difficulties usually appear in the biasing method, the simplicity and the compactness of the system. Similarly, in the case of MIMO systems, researchers either propose several isolation techniques between antennas [15] that may increase congestion or insert losses or simply enhance the antennas spacing between each other that seems to be very difficult using the compact

Received 6 March 2020, Accepted 14 May 2020, Scheduled 23 May 2020

* Corresponding author: Kadidiatou Diallo (Kadidiatou.diallo@univ-cotedazur.fr).

[1] Laboratoire d'Electronique Antennes et Téléommunications (LEAT-UMR CNRS), Université Côte d'Azur (UCA), Sophia Antipolis, France. [2] Laboratoire d'Informatique, Réseaux et Télécoms (LIRT-ESP), Université Cheikh Anta Diop (UCAD), Dakar, Sénégal.

available space. Indeed, studying the characteristic modes of the ground plane may solve the problem of spacing between antennas making the isolation very affordable.

In this paper, we propose a compact dual-band frequency tunable antenna system for mobile handsets. The system consists of an active dual-band (LTE-M/LTE-2500) PIFA antenna associated with a parasitic element, whose first resonance frequency is tunable between 700 MHz and 900 MHz by using varactor diode and another single PIFA antenna operating in LTE-2500 band in order to enable the 2×2 MIMO communication mode at this specified frequency band. The position and orientation of each of the two designed PIFAs were carefully chosen after studying the characteristic modes of the mobile phone chassis [16]. An overall view of the structure is shown in Figure 1 below.

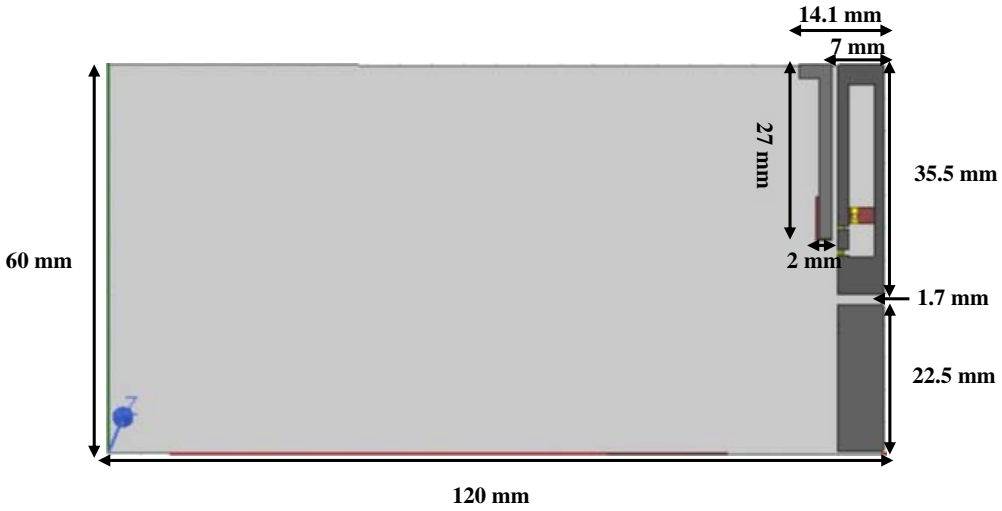

Figure 1. Overall view of the proposed antenna system.

2. STUDY OF THE CHARACTERISTICS MODES OF THE MOBILE PHONE CHASSIS

In MIMO systems, isolation between antenna ports is a very important feature that must be taken into consideration during the antenna system design. The study of the characteristic modes of the ground plane is a method that can be used to attain better isolation between the two antennas. Indeed, good port isolation can be obtained when these two antennas excite two isolated modes, separately. This method allows port isolation in MIMO systems without the use of any isolation technique. The theory of characteristic modes (TCM) was first introduced by Garbacz in 1965 [17] and can be defined as the orthogonal current modes laying over the surface of a conducting body, which depends on its shape and size. TCM is used for designing multi-mode antennas [18], widening antenna bandwidths, increasing the isolation between the antennas [19], etc.

Each characteristic mode is associated with a corresponding eigenvalue (λ_n) that provides information about its behavior at a given frequency. Resonant modes are modes that have their eigenvalues close to zero. Modes with positive eigenvalues are called inductive modes while those with negative eigenvalues are called capacitive modes. This information can also be obtained from the module and the argument of Modal Significance linked to the eigenvalue by Equation (1). The MS also determines the bandwidth of the mode.

$$\mathrm{MS} = \left| \frac{1}{1 + j\lambda_n} \right| \tag{1}$$

A mode can be excited by placing an antenna at the location where the electric field is maximum and oriented in the direction of the current flow. The simulation of the eigenvalues of a ground plane of dimension $60 \times 120\,\mathrm{mm}^2$ by using HFSS Ansys software between 2.4 GHz and 2.8 GHz is shown in Figure 2. It can be observed that the eigenvalues of the first four modes are close to zero. Whereby,

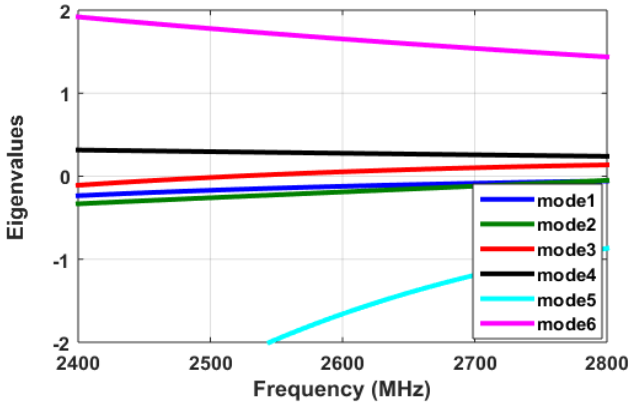

Figure 2. Simulation of the eigenvalues of the mobile phone chassis.

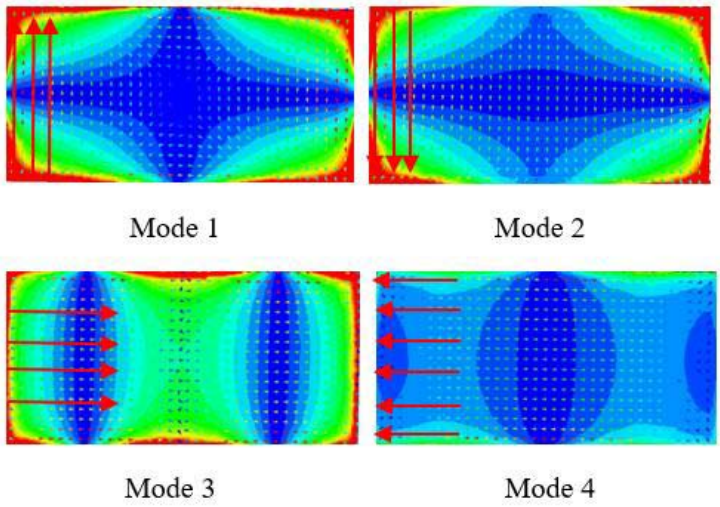

Figure 3. Electric field and surface current vector over the chassis at 2.6 GHz.

these modes will radiate when they are excited. Figure 3 shows the surface current vector and the electric field distribution over the ground plane at 2.6 GHz for modes 1, 2, 3, and 4. We notice from this figure two distinct behaviors of the pairs of mode (1, 2) and (3, 4). Modes 1 (odd mode) and 2 (even mode) present on the short edge of the ground plane have currents vector in opposition of phase; modes 3 (odd mode) and 4 (even mode) present on the long edge of the ground plane have electric fields in phase opposition (when one is maximum, the other is minimum). So if we ideally position and orient a PIFA antenna (known to have a more localized current distribution than monopoles), we can only excite in one instant t one of the modes. Thus, to design a MIMO system, we can place 2 PIFAs antennas either on the long edge or the short edge of the ground plane to excite a couple of modes, allowing us to obtain a good isolation. Therefore, to have a compact MIMO system, the two antennas can be placed at the short edge of the ground plane and must be oriented in a way that one of the two antennas excites mode 1, and the other excites mode 2, separately.

3. DESIGN OF FREQUENCY TUNABLE PIFA ANTENNA FOR LTE-M AND NB-LTE

In 5G systems, the frequency bandwidth [700–900 MHz] will be used for IoT standards (LTE-M and NB-IoT) for communications between connected devices. Thus, we propose a PIFA antenna which

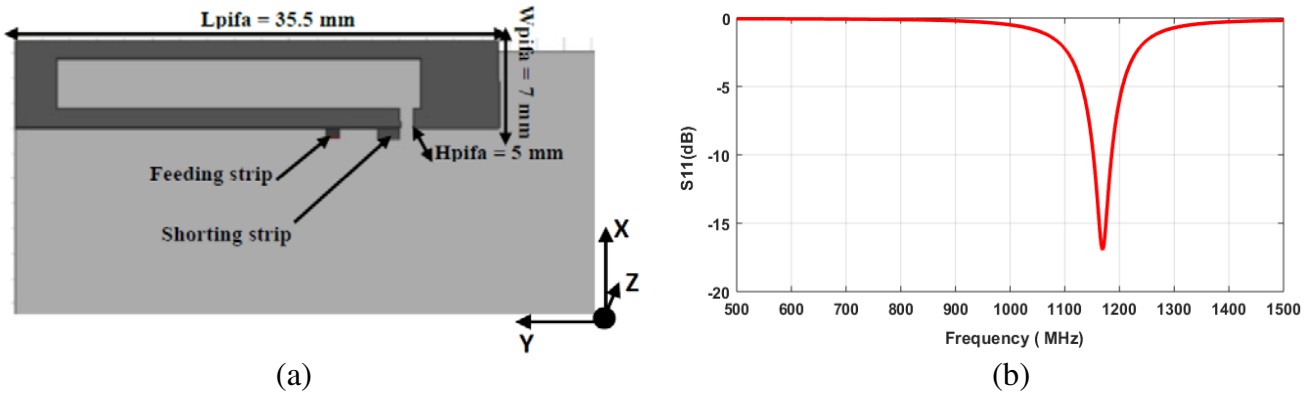

Figure 4. (a) Initial meandered PIFA, (b) simulation of S_{11} of the meandered PIFA.

can be integrated into a mobile terminal and cover the entire frequency band between 700 MHz and 900 MHz. The initial antenna structure is a meandered PIFA placed on the short edge of the ground (Figure 4(a)). Its dimensions are: $L_{\text{pifa}} = 35.5\,\text{mm}$, $W_{\text{pifa}} = 7\,\text{mm}$, and $H_{\text{pifa}} = 5\,\text{mm}$. The simulated reflection coefficient (Figure 4(b)) shows that this structure resonates at a frequency greater than 1 GHz. In addition, the bandwidth obtained is very low and will not cover the required 200 MHz.

To cover the entire 700 MHz–900 MHz band with this PIFA antenna without changing its dimensions, we decide to use a varactor diode that is modeled by its equivalent circuit (Figure 5). On the one hand, this varactor diode will add a capacitive load on the PIFA and thus lengthen its electrical length. On the other hand, by varying this capacity, the entire 700 MHz–900 MHz band can be covered.

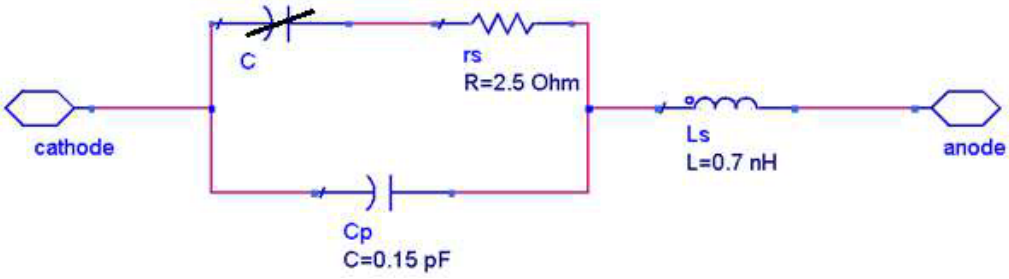

Figure 5. The varactor diode equivalent circuit.

In order to know the ideal position for the diode, we tried to place it in three different locations on the PIFA. We placed it first after the short circuit (position 1), then between the feeding strip and the short circuit (position 2), and finally, before the feeding strip (position 3). These different positions are illustrated in Figure 6. For each position, we plotted S_{11} with two diode capacitance values ($C = 0.5\,\text{pF}$ and $C = 1.05\,\text{pF}$). The S_{11} curves are shown in Figure 7. As can be observed from this figure, the ideal position for the varactor diode is position 1. Indeed, it is the position that gives a better frequency reconfiguration.

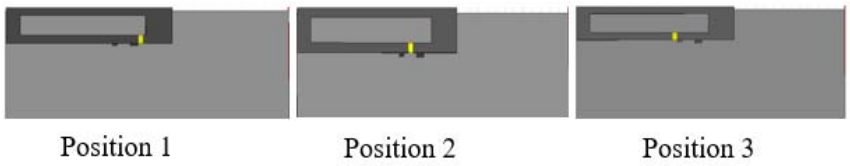

Figure 6. The PIFA antenna with different positions of the varactor diode.

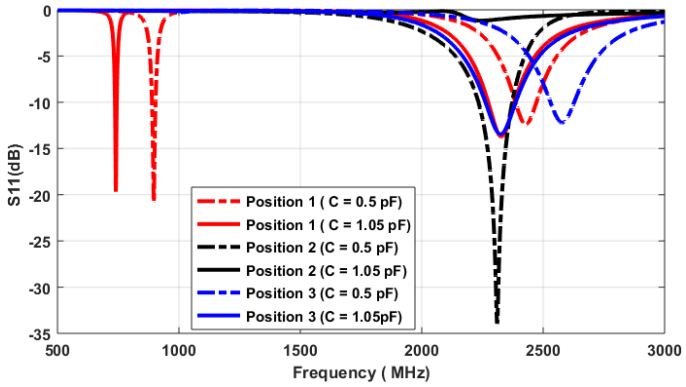

Figure 7. S_{11} for different positions of the varactor diode.

For the varactor diode to be well biased by the feeding pin, a 10 nF DC link capacitor is used on the PIFA to isolate the feeding strip from the short-circuit. Then, a parallel decoupling LC block ($L = 57$ nH and $C = 47$ pF) is connected to the feeding line to isolate the DC signal from the RF signal coming in the port input. The varactor diode and LC block are printed on a Duroid substrate with 0.787 mm thickness and 2.2 dielectric constant. This substrate is chosen so as not to influence the performance of the PIFA. Unlike the structures presented in [14], where the authors used two separate RF signal and DC bias ports, only one port is used in this work for the antenna feeding and the varactor diode bias thanks to the decoupling LC block. The structure of the reconfigurable PIFA is shown in Figure 8(a).

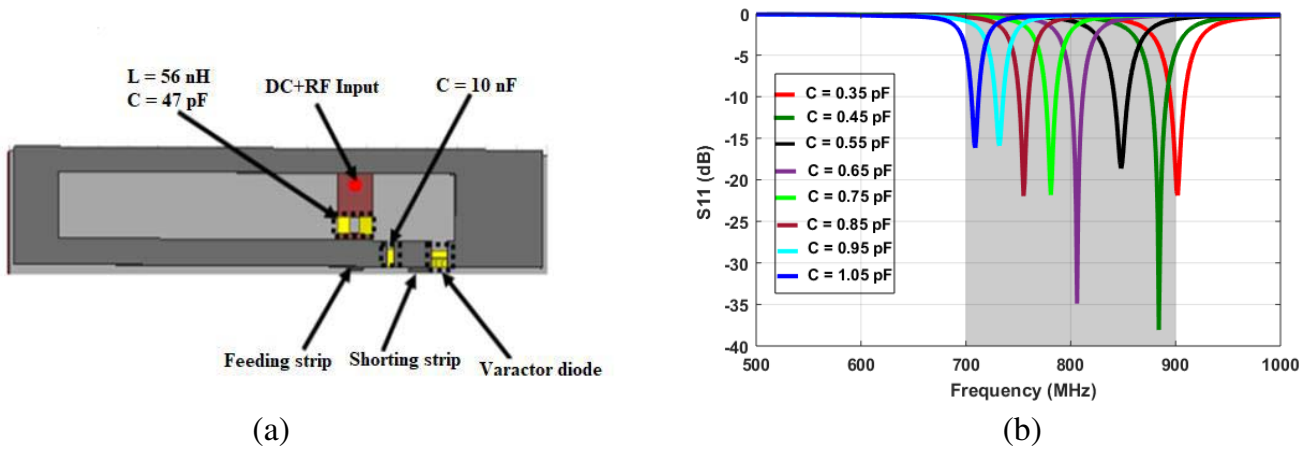

Figure 8. (a) Structure of the active reconfigurable PIFA, (b) simulation of reflection coefficient for C varying from 0.35 pF to 1.05 pF.

When the values of varactor diode capacitance are varied from 0.35 pF to 1.05 pF, it can be observed from Figure 8(b) that the PIFA resonance frequency is reconfigured from 700 MHz to 900 MHz.

4. DUAL-BAND FREQUENCY TUNABLE ANTENNA FOR LTE-M AND LTE-2500 APPLICATIONS

In order to know how the first higher order mode resonance frequency of the active PIFA varies when the diode capacitor changes, we have simulated the reflection coefficient for the minimum and maximum values of the diode capacitor (Figure 9). As can be seen, on the one hand, when the main resonance frequency varies, the first higher-order mode resonance frequency varies at the same time. On the other

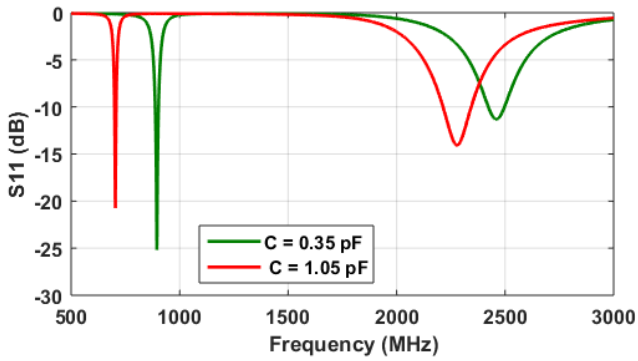

Figure 9. Variation of the first and second resonance frequencies of the PIFA with the capacitor.

hand, the bandwidth of the first higher order mode is not wide enough to cover the 200 MHz band required for mobile communications in the LTE 2500 band.

To have a fixed bandwidth of 200 MHz at high frequency, a parasitic PIFA is used. It is placed at 1 mm from the main PIFA (Figure 10(a)). This parasitic PIFA allows to widen the main PIFA's first higher order mode bandwidth. Thus, the whole structure forms a dual-band antenna whose low frequency is tunable from 700 MHz to 900 MHz, and the high frequency is fixed and covers the LTE band [2500–2700 MHz]. The simulation of the reflection coefficient of the dual-band antenna varying with frequency for different values of capacitor is shown in Figure 10(b). As shown, the resonant frequency of the antenna is reconfigurable in the first band, and at the same time a fixed bandwidth of 200 MHz is obtained in the second band. The high frequency bandwidth is given at −8 dB while the low frequency bandwidth is given at −6 dB.

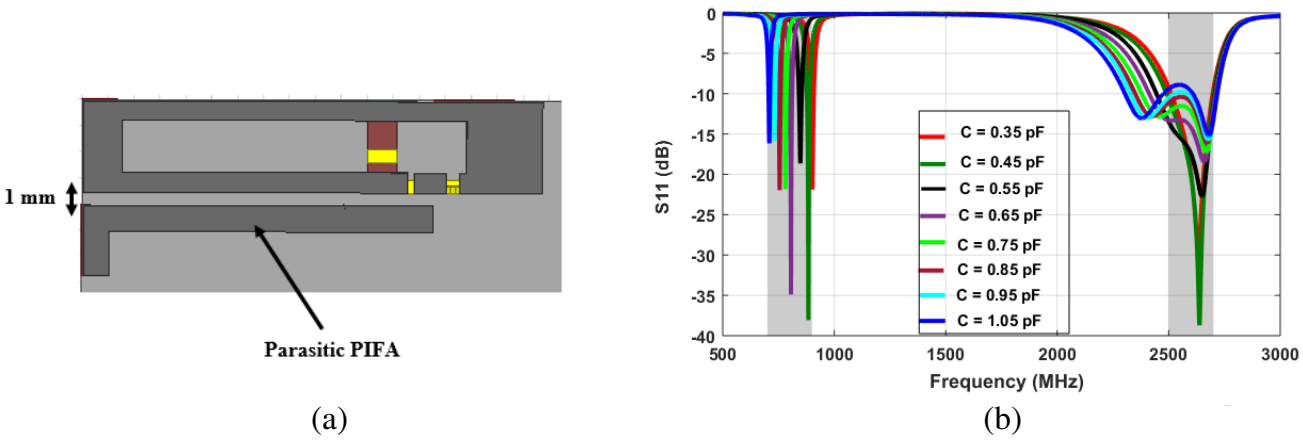

Figure 10. (a) Structure of the active dual-band reconfigurable PIFA, (b) simulation of S_{11} (dB) of the dual-band antenna for C varying from 0.35 pF to 1.05 pF.

5. THE MIMO SYSTEM DESIGN

Normally in LTE-2500 band for mobile phone, a MIMO system is required to increase the data rate. Thus, a single PIFA antenna of dimension $22.5 \times 7 \times 5\,\text{mm}^3$ was added to the ground plane to obtain multi-antenna system. It is optimized to operate only at the LTE-2500 band, unlike the first PIFA which has dual bands allowing working in LTE-700 and LTE-2500. The first antenna's position was chosen on the ground plane in Section 2, to excite at each time one of the two orthogonal modes, 1 or 2, which have currents vectors in opposition of phase following the short edge of the chassis. Thus, to

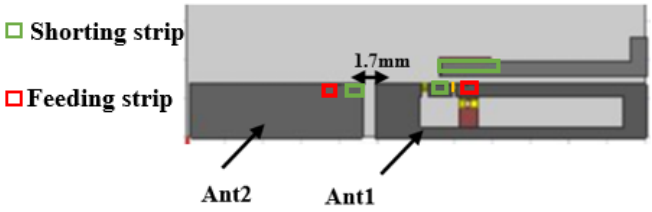

Figure 11. Structure of the MIMO system.

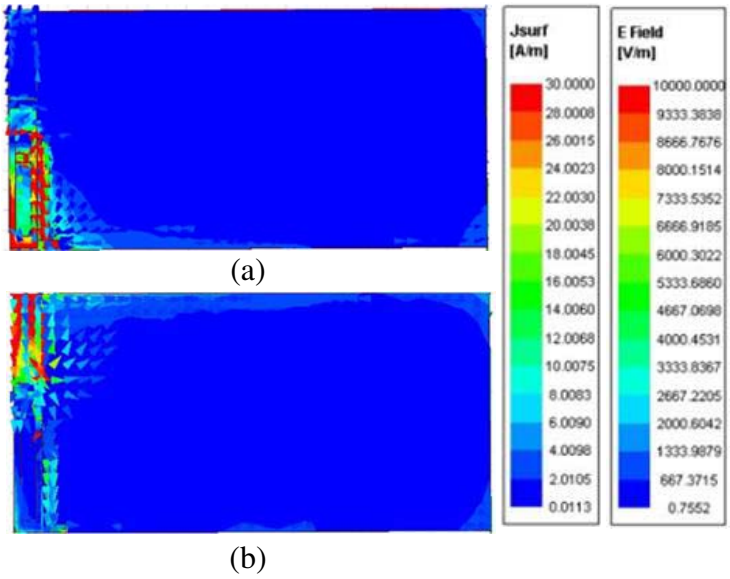

Figure 12. Visualization of the electric field (E field) and the surface current vector (J_{surf}) over the MIMO structure at 2.6 GHz when exciting (a) antenna 1 and (b) antenna 2.

have a good ports isolation, the second PIFA is then placed right next to the first PIFA in opposite orientation so that it can excite just the corresponding orthogonal mode (Figure 11). Figure 12 shows the distribution of the electric field and the surface current vector at 2.6 GHz, when only antenna1 is excited (a) and when only antenna 2 is excited (b).

Since the two antennas excite two orthogonal modes, good port isolation is achieved despite their small separating distance. Indeed, $|S_{21}|$ is better than -18 dB in the high band and falls below -27 dB in the low band. The simulation results of the S parameters of the MIMO system are represented in Figure 13 for different values of capacitance of the varactor diode. We can see that the low-frequency band (LTE-M) is tuned between 700 MHz and 900 MHz by changing the varactor value, while the high desired band (LTE-2500) is always covered regardless of the value of the varactor, with minimum isolation of 18 dB.

6. FABRICATION AND MEASUREMENT OF THE MIMO SYSTEM

A fabricated prototype of the MIMO system is presented in Figure 14. An SMV2020-079LF varactor diode is used. The measurement of S-parameters is performed by using a tee adapter to combine RF and DC signals into antenna 1 port. The curves of the measured S-parameters for different values of DC voltage, represented in Figure 15, show good agreement with the simulation ones for different values of capacitance which were shown before in Figure 13.

The measurement of the antenna total efficiency in the low band is performed using Wheeler cap method [20]. The efficiency was measured at the frequencies 745 MHz, 867 MHz, and 960 MHz

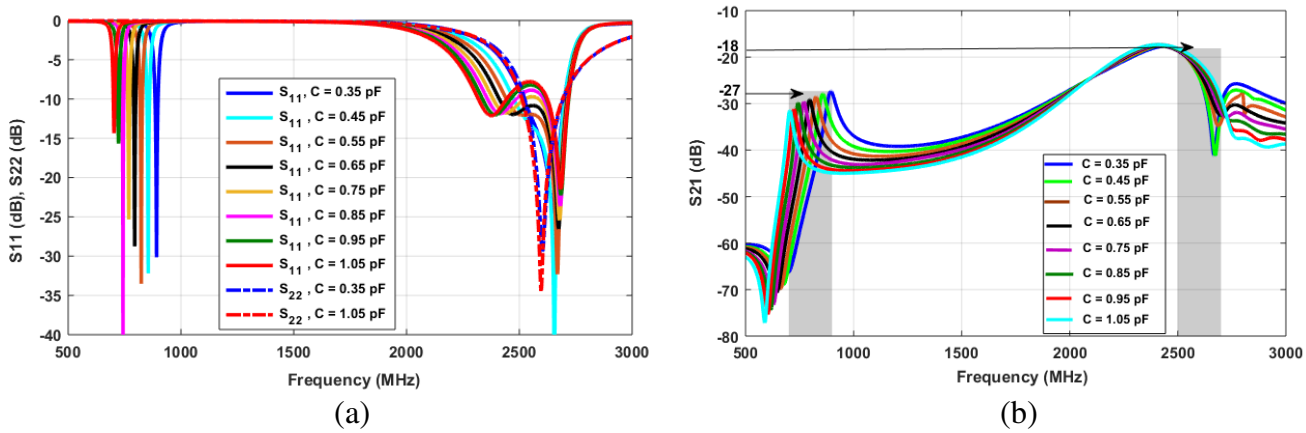

Figure 13. (a) Simulated reflection coefficients of the MIMO system, (b) simulated mutual coupling of the MIMO system.

Figure 14. The prototype of the MIMO system.

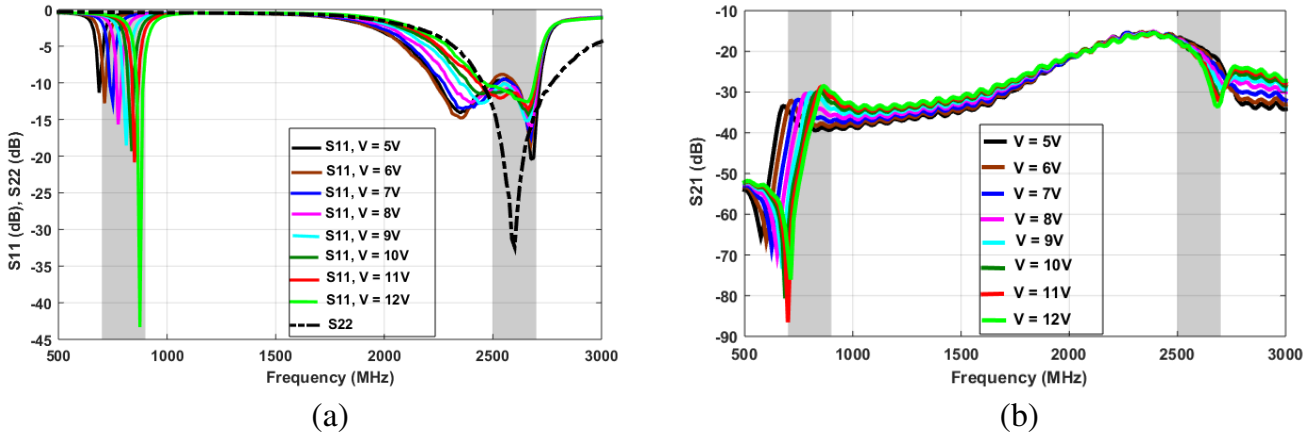

Figure 15. (a) Measured S_{11} and S_{22} of the MIMO system for different DC values, (b) measured S_{21} of the MIMO system for different DC values.

(Table 1). We have chosen to measure the efficiency in the low band up to a frequency higher than 900 MHz (960 MHz, corresponding to $V_{\mathrm{dc}} = 13.5\,\mathrm{V}$) to show that the efficiency of our reconfigurable PIFA antenna is improved when the frequency increases. Thus, despite the low values measured due to the series resistance of the diode, these efficiencies remain acceptable compared to the state of the art.

Table 1. Measured total efficiency in low band.

V_{dc} (V)	6.5	10.5	13.5
Frequency (MHz)	745	867	960
Efficiency (%)	17.4	31	46.7

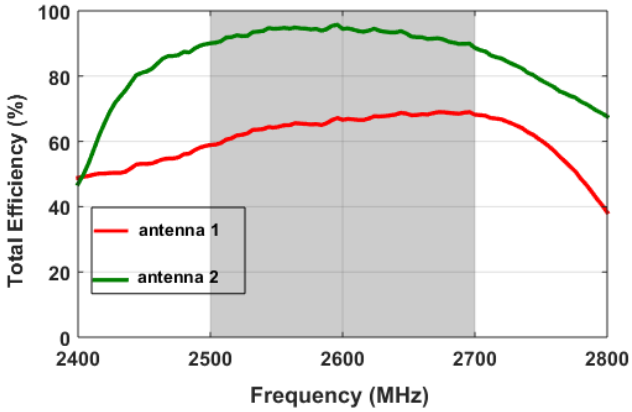

Figure 16. Measurement of total efficiency of the MIMO system.

Figure 16 shows the measured total efficiency of the MIMO system in the LTE-2500 band, performed in an anechoic chamber.

7. THE MIMO SYSTEM CHARACTERIZATION

7.1. Total Active Reflection Coefficient (TARC)

The TARC is defined as the ratio of the square root of the total reflected power divided by the square root of the total incident power [21, 22]. This parameter is used to define the effective operating bandwidth of MIMO systems. Figure 17 shows the calculated TARC using Equation (2) for $\theta = 0°$ and $\theta = 180°$, for the minimum and maximum values of the varactor diode.

$$\Gamma_a^t = \frac{\sqrt{|S_{11} + S_{12}e^{j\theta}|^2 + |S_{21} + S_{22}e^{j\theta}|^2}}{\sqrt{2}} \tag{2}$$

where θ is the phase of the incident power.

The curves of Figure 17 show that the bandwidth for MIMO applications is always covered in the LTE-2500 band at -8 dB.

7.2. Envelope Correlation Coefficient

The envelope correlation coefficient (ρ_e) is the parameter that provides information on the independence of signals in MIMO systems, and it varies from 0 to 1. A ρ_e equal to 0 indicates that signals are totally independent. The method of calculating envelope correlation (Equation (3)) requires 3D radiation pattern consideration [22, 23]. However, when the total efficiency of the antennas is high (good radiation efficiency, low isolation, and good matching) envelope correlation can be defined by a simpler form as in Equation (4). Equation (4) relates ρ_e to the S-parameters of the radiating elements [23]. Figure 18 shows the simulation of the envelope correlation coefficient using S-parameters and far fields, while its

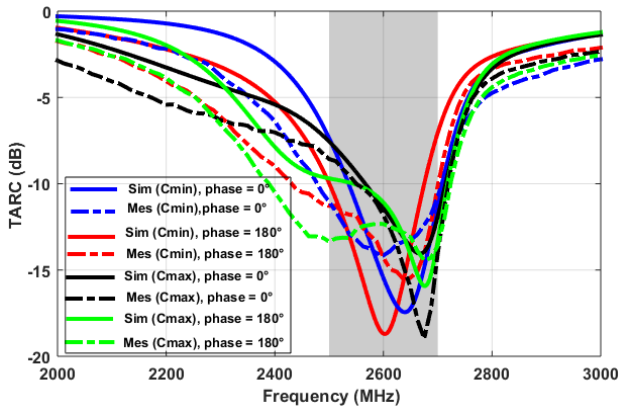

Figure 17. Simulated and measured TARC for $C_{\min}$ and $C_{\max}$.

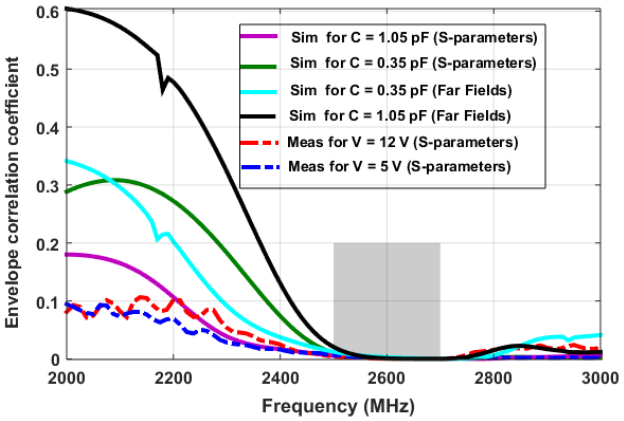

Figure 18. Simulation and measurement of the envelope correlation coefficient.

measurement results are done by just using S-parameters. Thus, we can see that in the high desired operation band, good isolation is obtained, and the envelope correlation is very low.

$$\rho_e = \frac{\left| \iint_{4\pi} \left[\vec{F}_1(\theta,\phi) \cdot \vec{F}_2^*(\theta,\phi) \right] d\Omega \right|^2}{\iint_{4\pi} \left| \vec{F}_1(\theta,\phi) \right|^2 d\Omega \iint_{4\pi} \left| \vec{F}_2(\theta,\phi) \right|^2 d\Omega} \tag{3}$$

$$\rho_e = \frac{\left| S_{11} * S_{12} + S_{21} * S_{22} \right|^2}{\left(1 - |S_{11}|^2 - |S_{21}|^2\right)\left(1 - |S_{22}|^2 - |S_{12}|^2\right)} \tag{4}$$

8. CONCLUSION

A compact dual-band frequency reconfigurable antenna system is presented in this article. It consists of one single LTE-2500 PIFA and an active reconfigurable dual-band PIFA associated with a parasitic PIFA. The dual-band PIFA frequency is tunable between 700 MHz and 900 MHz by using a single varactor diode simply biased from the RF port using a decoupling circuit to separate DC and RF signals while covering the LTE-2500 band as well. To minimize the mutual coupling between the two PIFAs and for the compactness of the system, TCM is used. The simulation and measurement of the antenna system show good agreement in its two operating frequency bands.

REFERENCES

1. Evans, D., "The internet of things. How the next evolution of the internet is changing everything," *Cisco White Paper*, 2011.
2. IoT Alliance Australia, Spectrum available for IoT, *Work Stream 4*, May 11, 2016.
3. Nokia, LTE-M-Optimizing LTE for the Internet of Things, *White Paper on LTE-M*, 2015.
4. Barreto, A. N., et al., "5G — Wireless communications for 2020," *Journal of Communication and Information Systems*, Vol. 31, No. 1, 146–163, 2016.
5. Ratasuk, R., N. Mangalvedhe, D. Bhatoolaul, and A. Ghosh, "LTE-M evolution towards 5G massive MTC," *JIEEE Globecom Workshops (GC Wkshps)*, 1–6, Singapore, 2017.
6. Huang, C., Y. C. Jiao, Z. B. Weng, and X. Li, "A planar multiband antenna based on CRLH-TL ZOR for 4G compact mobile terminal applications," *2018 International Workshop on Antenna Technology (iWAT)*, 1–3, Nanjing, 2018.

7. Chen, S.-C., J.-Y. Sze, Y. Chu, and C. Fu, "Reconfigurable LTE/WWAN antenna design," *2015 International Workshop on Electromagnetics: Applications and Student Innovation Competition (iWEM)*, 1–2, Hsin-Chu, Taiwan, 2015.
8. Lee, S. W. and Y. Sung, "Compact frequency reconfigurable antenna for LTE/WWAN mobile handset applications," *IEEE Transactions on Antennas and Propagation*, Vol. 63, No. 10, 4572–4577, Oct. 2015.
9. Rouissi, I., J. Floch, and H. Trabelsi, "Design of frequency reconfigurable PIFA antenna with floating ground plane," *Indian Journal of Science and Technology*, Vol. 11, No. 5, 1–11, Feb. 2018.
10. Yang, L., B. Cheng, Y. Zhu, and Y. Li, "Compact antenna with frequency reconfigurability for GPS/LTE/WWAN mobile handset applications," *International Journal of Antennas and Propagation*, Vol. 2016, Article ID 3976936, 8 pages, 2016.
11. Choi, M., H. Wi, B. Mun, Y. Yoon, H. Lee, and B. Lee, "A compact frequency reconfigurable antenna for LTE mobile handset applications," *International Journal of Antennas and Propagation*, Vol. 2015, Article ID 764949, 10 pages, 2015.
12. Young, M. W., S. Yong, and J. T. Bernhard, "A miniaturized frequency reconfigurable antenna with single bias, dual varactor tuning," *IEEE Transactions on Antennas and Propagation*, Vol. 63, 946–951, Jan. 2015.
13. Yu, Y., J. Xiong, H. Li, and S. He, "An electrically small frequency reconfigurable antenna with a wide tuning range," *IEEE Antennas and Wireless Propagation Letters*, Vol. 10, 103–106, Feb. 2011.
14. Keh, M. N. M., O. Quevedo-Teruel, and E. Rajo-Iglesias, "Reconfigurable loaded planar inverted-F antenna using varactor diodes," *IEEE Antennas and Wireless Propagation Letters*, Vol. 10, 466–468, May 2011.
15. Christina Josephine Malathi, A. and D. Thiripurasundari, "Review on isolation techniques in MIMO antenna systems," *Indian Journal of Science and Technology*, Vol. 9, No. 35, Sep. 2016.
16. Cabedo-Fabres, M., E. Antonino-Daviu, A. Valero-Nogueira, and M. Bataller, "The theory of characteristic modes revisited: A contribution to the design of antennas for modern applications," *IEEE Antennas and Propagation Magazine*, Vol. 49, No. 5, 52–68, Oct. 2007.
17. Garbacz, R. J., "Modal expansions for resonance scattering phenomena," *Proc. IEEE*, Vol. 53, No. 8, 856–864, 1965.
18. Antonino-Daviu, E., M. Cabedo-Fabrés, M. Ferrando-Bataller, and M. Gallo, "Design of a multimode MIMO antenna using the theory of characteristic modes," *Radioengineering*, Vol. 18, No. 4, 6, 2009.
19. Szini, I., A. Tatomirescu, and G. F. Pedersen, "On small terminal MIMO antennas, harmonizing characteristic modes with ground plane geometry," *IEEE Transactions on Antennas and Propagation*, Vol. 63, No. 4, 1487–1497, Apr. 2015.
20. Chair, R., K. M. Luk, and K. F. Lee, "Radiation efficiency analysis on small antenna by Wheeler cap method," *Microwave Opt. Technology Letters*, Vol. 33, No. 2, 112–113, Apr. 2002.
21. Chae, S. H., S. Oh, and S.-O. Park, "Analysis of mutual coupling, correlations, and TARC in WiBro MIMO array antenna," *IEEE Antennas Wireless Propagation Letters*, Vol. 6, 122–125, 2007.
22. Sharawi, M. S., "Printed MIMO antenna systems: Performance metrics, implementations and challenges," *FERMAT*, 11, 2014.
23. Votis, C., G. Tatsis, and P. Kostarakis, "Envelope correlation parameter measurements in a MIMO antenna array configuration," *IJCNS*, Vol. 3, No. 4, 350–354, 2010.